densed at −160° was C_2H_2 (6.8 mmol) while the fraction condensed at −130° contained only Si_2H_6 and ethynylsilane. Infrared spectral analysis of this mixture demonstrated that it consisted of 0.87 mmol of C_2HSiH_3 and 2.17 mmol of Si_2H_6. The fraction condensed at −95° (1.1 mmol) was a mixture of Si_3H_8 and ethynylvinylsilane while the fraction condensed at −78° was ethynyldivinylsilane (0.36 mmol). No vinylsilanes were detected.

In a similar experiment Si_2H_6 (3.36 mmol) and C_2H_3 (9.2 mmol) were pyrolyzed under the same conditions *without* SiH_4 removal. A small amount of H_2 was produced. The other products were separated by trap to trap distillation. The fraction condensed at −196° was SiH_4 (2.1 mmol) while that condensed at −160° was C_2H_2 (1.9 mmol). The fraction condensed at −130° (0.15 mmol) was a mixture of Si_2H_6, ethynylsilane, and vinylsilane. Condensed at −95° was a 1.62-mmol mixture of Si_3H_8, divinylsilane, and ethynylvinylsilane. Ethynyldivinylsilane (0.18 mmol) was condensed at −36°.

Pyrolysis of SiH_4 in the Presence of C_2H_2. 1. Reaction in Thermal Zone A (24 mm × 26 cm). Silane (4.43 mmol) and C_2H_2 (8.55 mmol) were pyrolyzed at 420° for 2 hr with a −119° bath on the "U" trap. After the reaction, 3.06 mmol of SiH_4 remained (condensed at −196°). The fraction condensed at −160° was C_2H_2 (7.7 mmol). The fraction condensed at −130° having passed a −95° trap (1.0 mmol) was analyzed by infrared spectroscopy to contain Si_2H_6, vinylsilane, and ethynylsilane in an approximate ratio of 1:1:1.

2. Reaction in Thermal Zone B (10 mm × 29 cm). Silane (5.75 mmol) and C_2H_2 (5.8 mmol) were pyrolyzed at 420° for 2 hr with the −119° cold trap. With similar separations, SiH_4 (5.3 mmol) and C_2H_2 (5.2 mmol) were found unreacted. The fraction (0.42 mmol) condensed at −130° (pass −95°) was analyzed by an infrared spectrum to contain Si_2H_6, vinylsilane, and ethynylsilane in an approximate ratio of 3:3:1.

3. Reaction in Thermal Zone C (10 mm × 10 cm). Silane (5.25 mmol) and C_2H_2 (5.73 mmol) were pyrolyzed at 440° for 2 hr. The reactants found after the pyrolysis were SiH_4 (5.16 mmol) and C_2H_2 (5.66 mmol). The product fraction (0.2 mmol) condensed at −130° (pass −95°) contained Si_2H_6, vinylsilane, and ethynylsilane in an approximate ratio of 15:50:1 as analyzed by infrared spectroscopy. In a similar experiment this last ratio was found to be approximately 12:20:1.

Acknowledgment. The authors are indebted to W. D. Jones for discussions concerning the orbital symmetry arguments.

Registry No. SiH_4, 7803-62-5; Si_2H_6, 1590-87-0; SiH_2, 13825-90-6; SiH_3, 13765-44-1; $HC{\equiv}CSiH_3$, 1066-27-9; C_2H_2, 74-86-2.

References and Notes

(1) J. H. Purnell and R. Walsh, *Proc. Roy. Soc. London, Ser. A*, 543 (1966).

(2) M. A. Ring, M. J. Puentes, and H. E. O'Neal, *J. Am. Chem. Soc.*, **92**, 4845 (1970).

(3) P. John and J. H. Purnell, *J. Organomet. Chem.*, **29**, 233 (1971).

(4) D. G. White and E. G. Rochow, *J. Am. Chem. Soc.*, **76**, 3897 (1954).

(5) (a) M. E. Volpin, Yu. D. Koreshkov, V. G. Dulova, and D. N. Kursanov, *Tetrahedron*, **18**, 107 (1962); (b) R. West and R. E. Bailey, *J. Am. Chem. Soc.*, **85**, 2871 (1963); (c) F. Johnson, R. S. Gohlke, and W. H. Nasutavicus, *J. Organomet. Chem.*, **3**, 233 (1965); (d) W. H. Atwell and D. R. Weyenberg, *J. Am. Chem. Soc.*, **90**, 3438 (1968); (e) W. H. Atwell and J. G. Uhlman, *J. Organomet. Chem.*, **52**, C21 (1973); (f) T. J. Barton and J. A. Kilgour, *J. Am. Chem. Soc.*, **96**, 7150 (1974).

(6) R. G. Pearson, *J. Am. Chem. Soc.*, **94**, 8287 (1972).

(7) G. Herzberg, "Molecular Spectra and Molecular Structure", Reinhold, New York, N.Y., 1966, p 584.

(8) I. Dubois, *Can. J. Phys.*, **46**, 2485 (1968).

(9) S. R. Gunn and L. G. Green, *J. Phys. Chem.*, **65**, 779 (1961); P. John and J. H. Purnell, *J. Chem. Soc., Faraday Trans. 1*, **69**, 1455 (1973).

(10) K. Fukui, *Acc. Chem. Res.*, **4**, 57 (1971); R. G. Pearson, *ibid.*, **4**, 152 (1971).

(11) P. Estacio, M. D. Sefcik, E. K. Chan, and M. A. Ring, *Inorg. Chem.*, **9**, 1068 (1970).

(12) M. Bowery and J. H. Purnell, *J. Am. Chem. Soc.*, **92**, 2594 (1970).

(13) O. F. Zeck, Y. Y. Su, G. P. Gennaro, and Y. N. Tang, *J. Am. Chem. Soc.*, **96**, 5967 (1974).

(14) R. L. Jenkins, R. A. Kedrowski, L. E. Elliott, D. C. Tappen, D. J. Schyler, and M. A. Ring, *J. Organomet. Chem.*, **86**, 347 (1975).

(15) R. B. Reeves, R. E. Wilde, and D. W. Robinson, *J. Chem. Phys.*, **40**, 127 (1964).

(16) E. J. Spanier and A. G. MacDiarmid, *Inorg. Chem.*, **1**, 432 (1962).

(17) S. G. Frankiss, *Spectrochim. Acta*, **22**, 300 (1966).

Contribution from the Department of Chemistry,
Michigan State University, East Lansing, Michigan 48824

Microwave Spectrum and Dipole Moment of Methyldifluorophosphine–Borane[1,2]

ROBERT A. CRESWELL, R. A. ELZARO, and R. H. SCHWENDEMAN*

Received February 25, 1975 AIC50142W

The microwave spectra of $CH_3PF_2{\cdot}{}^{11}BH_3$, $CH_3PF_2{\cdot}{}^{10}BH_3$, $CH_3PF_2{\cdot}{}^{11}BD_3$, and $CH_3PF_2{\cdot}{}^{10}BD_3$ have been assigned. Stark effect measurements gave the following values for the dipole moment and its components: $\mu_a = 3.52$ (5) D, $\mu_b = 1.76$ (5) D, $\mu_c = 0.0$ D, and $\mu = 3.94$ (5) D. The absence of resolvable internal rotation splittings in the ground state yields lower limits of about 2000 cal/mol for the barriers to both CH_3 and BH_3 group internal rotation. By judicious transfer of structural parameters from related molecules r(P–B) was estimated to be 1.84 ± 0.02 Å.

Introduction

Compounds containing P–B dative bonds have recently received considerable attention.[3–9] One particularly interesting facet of their properties is the large variation in their stabilities with respect to dissociation: $H_3P{\cdot}BH_3$[6] is completely dissociated at 273 K, and $F_3P{\cdot}BH_3$[3] is extensively dissociated at the same temperature, whereas $(CH_3)_3P{\cdot}BH_3$[5] may be heated to about 473 K without appreciable dissociation. Attempts to correlate stability with the length of the P–B bond have met with little success; the values for this parameter in the above compounds are 1.937 (5), 1.836 (12), and 1.901 (7) Å, respectively.

The preparation of methyldifluorophosphine–borane, $CH_3PF_2{\cdot}BH_3$, has been recently reported by Foester and Cohn.[10] They studied a series of base displacement reactions and found that CH_3PF_2 was surprisingly basic toward BH_3, and they suggested that an unexpected structural deformation upon adduct formation might be the explanation of this observation. We have recently reported a study of the microwave spectrum of CH_3PF_2[11] as a part of our interest in difluorophosphine derivatives.[12–15] As a continuation of this work, and in an attempt to investigate the speculation of Foester and Cohn about the structure of the complex, we have obtained the microwave spectrum of $CH_3PF_2{\cdot}BH_3$.

Experimental Section

The samples of $CH_3PF_2{\cdot}BH_3$ and $CH_3PF_2{\cdot}BD_3$ were obtained from Dr. K. Cohn. The spectra were recorded at about 220 K and at room temperature with an Hewlett-Packard 8460A microwave spectrometer in the 18–40-GHz frequency region. The spectra of the ^{11}B and ^{10}B isotopic species were assigned in their natural isotopic abundance. The estimated errors in the frequency measurements are ±0.1 MHz.

Spectrum

A projection of the molecule in the *ab* plane is shown in Figure 1. A trial set of rotational constants was calculated from a structure obtained by selection of structural parameters

Table I. Comparison of Observed[a] and Calculated[b] Frequencies of Rotational Transitions in Methyldifluorophosphine–Borane

Transition	$CH_3PF_2\cdot{}^{11}BH_3$	$CH_3PF_2\cdot{}^{10}BH_3$	$CH_3PF_2\cdot{}^{11}BD_3$	$CH_3PF_2\cdot{}^{10}BD_3$
3_{03}–4_{04}	28,429.52 (0.17)	29,189.94 (0.15)		
3_{13}–4_{14}	28,315.05 (0.14)	29,098.13 (0.14)		
3_{12}–4_{13}	28,904.92 (0.31)	29,697.10 (0.15)		
3_{22}–4_{23}	28,645.29 (0.15)		25,581.18 (0.06)	
3_{21}–4_{22}	28,882.86 (0.16)		25,714.17 (0.08)	
3_{31}–4_{32}	28,715.01 (0.03)			
4_{04}–5_{05}	35,434.98 (0.01)	36,386.00 (–0.07)	31,746.83 (–0.03)	
4_{14}–5_{15}	35,359.39 (0.03)	36,333.29 (–0.01)	31,619.57 (0.07)	
4_{13}–5_{14}	36,056.16 (0.06)	37,023.14 (–0.05)	32,234.93 (0.02)	
4_{23}–5_{24}	35,771.60 (–0.04)	36,759.57 (–0.03)	31,958.55 (–0.10)	32,705.33 (0.10)
4_{22}–5_{23}	36,158.19 (0.03)	37,206.60 (0.03)	32,201.61 (–0.03)	32,983.32 (0.19)
4_{32}–5_{33}	35,901.09 (–0.10)	36,915.60 (0.02)	32,029.65 (–0.02)	32,788.54 (0.30)
4_{31}–5_{32}	35,965.72 (–0.17)	37,011.35 (–0.05)		32,915.84 (–0.21)
4_{41}–5_{42}	35,896.24 (–0.21)	36,915.96 (–0.10)		
4_{40}–5_{41}	35,898.70 (–0.31)			
4_{04}–5_{15}	35,517.35 (0.01)	36,431.29 (–0.09)		
4_{13}–5_{24}	36,906.42 (–0.08)			
4_{23}–5_{32}	39,127.62 (0.12)			
4_{22}–5_{33}	38,667.36 (–0.09)			
4_{41}–5_{50}			39,616.49 (0.00)	
5_{33}–6_{34}				39,351.33 (–0.18)
5_{32}–6_{33}				39,422.28 (–0.13)

[a] In MHz. Estimated uncertainties are ±0.1 MHz. [b] Values in parentheses are observed minus calculated frequencies in MHz.

Table II. Inertial Constants of Methyldifluorophosphine–Borane

	$CH_3PF_2\cdot{}^{11}BH_3$	$CH_3PF_2\cdot{}^{10}BH_3$	$CH_3PF_2\cdot{}^{11}BD_3$	$CH_3PF_2\cdot{}^{10}BD_3$
A/MHz[a]	4193.95	4198.83	4046.13	4047.16
B/MHz	3659.55	3762.36	3262.63	3340.56
C/MHz	3507.26	3605.20	3135.43	3207.98
I_a/u Å^2 [b]	120.5011	120.3611	124.9037	124.8718
I_b/u Å^2	138.0978	134.3242	154.8981	151.2847
I_c/u Å^2	144.0943	140.1795	161.1824	157.5370
P_{aa}/u Å^2 [c]	80.8455	77.0713	95.5884	91.9749
P_{bb}/u Å^2	63.2488	63.1082	65.5940	65.5621
P_{cc}/u Å^2	57.2523	57.2528	59.3097	59.3097[d]

[a] Estimated uncertainty in rotational constants: ±0.05 MHz. [b] Rotational constant/MHz = 505,376/(moment of inertia/u Å^2). [c] $P_{aa} = \frac{1}{2}(I_b + I_c - I_a)$, etc. [d] Assumed.

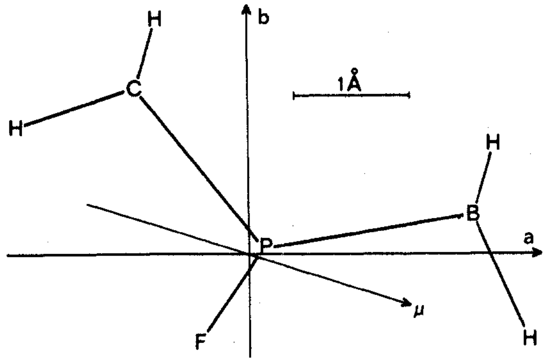

Figure 1. Projection of $CH_3PF_2\cdot BH_3$ in its *ab* plane of symmetry showing the orientation of the dipole moment vector. The dipole moment vector points from plus to minus charge.

from CH_3PF_2[11] and $HPF_2\cdot BH_3$.[4] This structure predicted that both *a*- and *b*-type rotational transitions would be observed, with the spectrum being dominated by *b*-type Q-branch transitions. The observed spectrum was consistent with this prediction, its major feature being strong Q-branch series with band heads having separations of about 1240 and 1700 MHz for the $^{11}BH_3$ and $^{11}BD_3$ isotopic species, respectively. However, the assignment of the spectra was achieved with the less obvious low-*J* *a*- and *b*-type R-branch transitions. The corresponding transitions for the $^{10}BH_3$ and $^{10}BD_3$ species were predicted to lie in dense Q-branch frequency regions, and even with the 20% abundance of ^{10}B it was not possible to assign these transitions in the Stark spectrum. Their assignment was however readily achieved with the use of the radiofrequency microwave double-resonance technique described by Wodarczyk and Wilson.[16]

Table III. Stark Effect and Dipole Moment[a] of Methyldifluorophosphine–Borane

		$d\nu/dE^2$ [b]	
Transition	|M|	Obsd[c]	Calcd
4_{04}–5_{05}	1	3.202 (16)	3.196
	2	17.97 (8)	18.02
	3	42.76 (20)	42.74
4_{14}–5_{15}	1	3.853 (18)	3.816
	2	20.14 (10)	20.15
	3	47.10 (22)	47.35

$\mu_a^2 = 12.390\ D^2$ $\mu_a = 3.52\ (5)\ D$
$\mu_b^2 = 3.115\ D^2$ $\mu_b = 1.76\ (5)\ D$
$\mu_c^2 = 0.0\ D^2$ (assumed) $\mu = 3.94\ (5)\ D$

[a] Relative to μ(OCS) = 0.7152 D. [b] Hz/(V/cm)^2. [c] Numbers in parentheses are experimental uncertainties on the last digit(s) quoted.

Table IV. Structural Parameters[a] of $CH_3PF_2\cdot BH_3$

Parameter	Value[b]	Parameter	Value[b]
C–H	[1.093]	P–B	1.841 (20)
P–F	[1.552]	B–H	1.209 (10)
P–C	[1.800]		
∠HCH	[109.5]	∠BPF	116.1 (20)
∠HBH	114.3 (10)	∠CPF	101.9 (20)
∠FPF	99.8 (20)	∠PCH	109.4 (20)
∠BPC	118.2 (20)	∠PBH	104.0 (10)

[a] Distances are in angstroms; angles are in degrees. [b] Values in brackets are assumed; values in parentheses are estimated uncertainties.

Table V. Dipole Moments of Phosphines and Their BH_3 Adducts

Phosphine	Dipole moment/D	Ref	BH_3 adduct dipole moment/D	Ref
PH_3	0.58	21	4.00	6
CH_3PH_2	1.10	20	4.66	5
$(CH_3)_2PH$	1.23	22	4.85	9
$(CH_3)_3P$	1.19	23	4.99	5
PF_3	1.03	25	1.64	3
HPF_2	1.32	24	2.50	4
CH_3PF_2	2.06	11	3.95	This work

The observed transitions are quite broad but no splittings which could definitely be assigned to either internal rotation or nuclear quadrupole coupling were observed. The measured transitions and their deviations from a least-squares rigid-rotor fit are listed in Table I. The corresponding rotational constants, moments of inertia, and planar second moments are given in Table II. No *b*-type low-*J* transitions could be measured for the $^{10}BD_3$ species so its measured *a*-type transitions were fit by constraining P_{cc} to its value in the $^{11}BD_3$ species.

Dipole Moment

Quantitative measurements of the Stark effect were made on three M components of each of two transitions in the spectrum of $CH_3PF_2\cdot{}^{11}BH_3$. These data are summarized in Table III. Their analysis yielded the following dipole moment components: $\mu_a = 3.52$ (5) D, $\mu_b = 1.76$ (5) D, $\mu_c = 0.0$ D, and $\mu = 3.94$ (5) D relative to μ(OCS) = 0.7152 D.[17] The dipole moment vector makes an angle of 26.6° with the *a* principal axis. Although the sign of this angle and the direction of the dipole moment vector are not determinable from these data, the orientation of the dipole moment is most likely that shown in Figure 1.

Structure

The available data are not sufficient to permit a complete determination of the structure of $CH_3PF_2\cdot BH_3$. Probably the best that can be done is to show that a structure consistent with the structures determined for other phosphine–borane adducts is compatible with the experimental rotational constants.

The presence of a plane of symmetry is strongly supported by the equality, within experimental uncertainty, of P_{cc} for the $CH_3PF_2\cdot{}^{11}BH_3$ and $CH_3PF_2\cdot{}^{10}BH_3$ isotopic species. With this plane of symmetry and the assumption of untilted, symmetric methyl and borane groups in the doubly staggered configuration of Figure 1, ten parameters are required to specify the structure of $CH_3PF_2\cdot BH_3$. Since we have essentially only eight pieces of data, from the isotopic species assigned, at least two further assumptions are necessary in order to calculate a structure from these data. We have chosen to assume a C–H bond length of 1.093 Å and an ∠HCH angle of 109.5°. Also, to provide a check of the internal consistency of the calculation, we have fixed the P–F bond length to be 1.552 Å, its value in $HPF_2\cdot BH_3$.[4] The computer program STRFTQ[18] was used to adjust the parameters B–H, P–B, P–C, ∠HBP, ∠BPC, ∠FPF, and ∠BPF to fit the moments of inertia in Table II. Unfortunately, the P–B and P–C distances are highly correlated with respect to this data set, and only their sum is well determined to be 3.642 (10) Å. The structure given in Table IV was obtained by fixing the P–C distance to be 1.80 Å by comparison with the structures of CH_3PF_2,[11] CH_3PH_2,[19] and $CH_3PH_2\cdot BH_3$.[5] The uncertainties given in Table IV are intended to reflect the changes caused by reasonable variation of the assumed parameters; however, no allowance for a possible tilt of either the CH_3 or BH_3 groups has been included. The structure given in Table IV must not be regarded as a definitive structure for $CH_3PF_2\cdot BH_3$ but as the most probable one based on the available inertial data and comparison with other phosphine–borane adducts.

Discussion

A comparison of the dipole moments of CH_3PF_2[11] and $CH_3PF_2\cdot BH_3$ with the dipole moments of other phosphines and their borane adducts is given in Table V.

Table VI presents a comprehensive summary of the structural parameters of all phosphine–borane adducts and the free phosphine molecules which have been studied in the gas phase to date. From the data in this table one can readily see that adduct formation is always accompanied by a

Table VI. Structural Parameters[a] of Phosphines and Their Borane Adducts

	PH_3	$PH_3\cdot BH_3$	CH_3PH_2	$CH_3PH_2\cdot BH_3$	$(CH_3)_2PH$	$(CH_3)_2PH\cdot BH_3$	$(CH_3)_3P$	$(CH_3)_3P\cdot BH_3$	PF_3	$PF_3\cdot BH_3$	PF_2H	$PF_2H\cdot BH_3$	CH_3PF_2	$CH_3PF_2\cdot BH_3$
P–H	1.421	1.399 (3)	1.423 (7)	1.404 (6)	1.419 (5)	1.414 (9)					1.412 (6)	1.409 (4)		
P–F									1.570 (2)	1.538 (8)	1.582 (2)	1.552 (6)	1.582 (5)	[1.552]
P–C			1.858 (3)	1.809 (6)	1.848 (3)	1.813 (10)	1.843 (3)	1.819 (10)					1.825 (2)	[1.800]
B–H_a		1.212 (2)		1.229 (22)		1.216 (5)		1.212 (10)		1.207 (6)		1.226 (5)		1.209 (10)
B–H_s		1.212 (2)		1.234 (23)		1.212 (5)		1.212 (10)		1.207 (6)		1.200 (7)		1.209 (10)
P–B		1.937 (5)		1.906 (6)		1.898 (10)		1.901 (7)		1.836 (12)		1.832 (9)		1.841 (20)
∠XPX[b]	93.5	101.3 (2)	93.4 (10)	99.9 (4)	99.7 (3)	105.5 (10)	98.9 (2)	105.0 (4)	97.8 (2)	99.8 (10)	99.0 (2)	100.0 (5)	98.4 (5)	99.8 (20)
∠XPY[c]			98.4 (10)	103.2 (6)	97.0 (3)						96.3 (5)	98.6 (2)	97.8 (5)	101.9 (20)
∠BPH		116.9 (2)		116.3 (6)		118.1 (40)						120.1 (6)		
∠BPF										118.0 (10)		117.7 (3)		116.1 (20)
∠BPC				115.7 (4)		114.6 (10)								118.2 (20)
∠H_aBH_a		114.6 (2)		112.3 (12)		113.2 (5)		113.5 (5)		115.0 (10)		112.7 (5)		114.3 (10)
∠H_sBH_a		114.6 (2)		116.1 (8)		113.3 (5)		113.5 (5)		115.0 (10)		115.9 (4)		114.3 (10)
∠PBH_s		103.6 (2)		104.2 (10)		104.9 (4)		104.7 (5)		103.2 (10)		109.9 (3)		104.0 (10)
∠PBH_a		103.6 (2)		102.9 (6)		104.8 (4)		104.7 (5)		103.2 (10)		99.9 (3)		104.0 (10)
Ref	28	6	19	5	22	9	26	5	27	3	24	4	11	This work

[a] Distances are in angstroms; angles are in degrees. Numbers in parentheses are estimated uncertainties. Values in brackets are assumed values. Methyl group geometries are not given but all C–H values are close to 1.093 Å and all ∠HCH values are close to 109.5°. [b] ∠XPX represents ∠HPH, ∠FPF, or ∠CPC as appropriate. [c] ∠XPY represents ∠HPF, ∠HPC, or ∠FPC as appropriate.

Table VII. Barriers to Internal Rotation in Phosphines and Phosphine–Borane Adducts

Compd	Barrier/(cal/mol) CH_3	BH_3	Ref
CH_3PH_2	1960		20
$CH_3PH_2\cdot BH_3$	2490	1570	29
$PH_3\cdot BH_3$		2470	6
$PF_3\cdot BH_3$		3240	3
CH_3PF_2	2300		11
$CH_3PF_2\cdot BH_3$	>2000	>2000	This work
$HPF_2\cdot BH_3$		3600–4500	4

shortening of the bond lengths between the phosphorus atom and its attached atoms and also by a flattening of the pyramid of which the phosphorus atom is the apex. The limited structural data on $CH_3PF_2\cdot BH_3$ are consistent with these two general observations. The P–B bond lengths seem to fall into two groups, greater than 1.90 Å when hydrogen atoms or methyl groups are bonded to the phosphorus and about 1.84 Å when fluorine atoms are attached to the phosphorus. The data on $CH_3PF_2\cdot BH_3$ also exhibit this effect. These observations about the structures of phosphine–borane adducts have been made before.[5] They are repeated here to show that the data for $CH_3PF_2\cdot BH_3$ are consistent with the data for other members of this class of compounds. The structure changes which occur in the phosphine upon adduct formation are consistent with the predictions of elementary bonding models, whereas there seems to be no uniquely compelling explanation for the variation of the observed P–B bond lengths and stabilities of the adducts.[5] While this study of the structure of $CH_3PF_2\cdot BH_3$ is by no means complete, the results do not appear to support the speculation of Foester and Cohn[10] concerning an unusual structural deformation in CH_3PF_2 upon adduct formation.

Table VII summarizes barriers to internal rotation in related compounds. The absence of resolvable splittings in the ground vibrational state of $CH_3PF_2\cdot BH_3$ places lower limits of about 2000 cal/mol on both the CH_3 and BH_3 barriers to internal rotation. In CH_3PH_2 formation of the BH_3 adduct has increased the barrier to CH_3 internal rotation by 530 cal/mol, and in $PH_3\cdot BH_3$ the substitution of a methyl group on the phosphorus has lowered the barrier to BH_3 group internal rotation by 900 cal/mol. Similar changes applied to the data on CH_3PF_2 and PF_2BH_3 predict values of 2830 and 2340 cal/mol, respectively, for CH_3 and BH_3 group internal rotation barriers in the present compound. These predictions are quite crude, but they do serve to show that the experimental observation that both barriers in the present compound are greater than 2000 cal/mol is consistent with the data on related compounds.

Registry No. $CH_3PF_2\cdot{}^{11}BH_3$, 55606-68-3; $CH_3PF_2\cdot{}^{11}BD_3$, 55606-69-4; $CH_3PF_2\cdot{}^{10}BH_3$, 55606-70-7; $CH_3PF_2\cdot{}^{10}BD_3$, 55606-69-4.

References and Notes

(1) This work was supported in part by grants from the National Science Foundation.

(2) A preliminary account of this work was presented at the Symposium on Molecular Structure and Spectroscopy, Columbus, Ohio, June 1974.

(3) R. L. Kuczkowski and D. R. Lide, Jr., *J. Chem. Phys.*, **46**, 357 (1967).

(4) J. P. Pasinski and R. L. Kuczkowski, *J. Chem. Phys.*, **54**, 1903 (1971).

(5) P. S. Bryan and R. L. Kuczkowski, *Inorg. Chem.*, **11**, 553 (1972).

(6) J. R. Durig, Y. S. Li, L. A. Carriera, and J. D. Odom, *J. Am. Chem. Soc.*, **95**, 2491 (1973).

(7) J. D. Odom, B. A. Hudgens, and J. R. Durig, *J. Phys. Chem.*, **77**, 1972 (1973).

(8) J. D. Odom, S. Riethmiller, S. J. Meischen, and J. R. Durig, *J. Mol. Struct.*, **20**, 471 (1974).

(9) J. R. Durig, B. A. Hudgens, Y. S. Li, and J. D. Odom, *J. Chem. Phys.*, **61**, 4890 (1974).

(10) R. Foester and K. Cohn, *Inorg. Chem.*, **11**, 2590 (1972).

(11) E. G. Codding, R. A. Creswell, and R. H. Schwendeman, *Inorg. Chem.*, **13**, 856 (1974).

(12) A. H. Brittain, J. E. Smith, P. L. Lee, K. Cohn, and R. H. Schwendeman, *J. Am. Chem. Soc.*, **93**, 6772 (1971).

(13) A. H. Brittain, J. E. Smith, and R. H. Schwendeman, *Inorg. Chem.*, **11**, 39 (1972).

(14) P. L. Lee, K. Cohn, and R. H. Schwendeman, *Inorg. Chem.*, **11**, 1917 (1972).

(15) E. G. Codding, C. E. Jones, and R. H. Schwendeman, *Inorg. Chem.*, **13**, 178 (1974).

(16) F. J. Wodarczyk and E. B. Wilson, *J. Mol. Spectrosc.*, **37**, 445 (1971).

(17) J. S. Muenter, *J. Chem. Phys.*, **48**, 4544 (1968).

(18) R. H. Schwendeman, in "Critical Evaluation of Chemical and Physical Structural Information", D. R. Lide, Jr., and M. A. Paul, Ed., National Academy of Sciences, Washington, D.C., 1974, Chapter III.3.

(19) L. S. Bartell, *J. Chem. Phys.*, **32**, 832 (1960).

(20) T. Kojima, E. L. Breig, and C. C. Lin, *J. Chem. Phys.*, **35**, 2139 (1961).

(21) C. A. Burrus, *J. Chem. Phys.*, **28**, 427 (1958).

(22) R. Nelson, *J. Chem. Phys.*, **39**, 2382 (1963).

(23) D. R. Lide and D. E. Mann, *J. Chem. Phys.*, **29**, 914 (1958).

(24) R. L. Kuczkowski, *J. Am. Chem. Soc.*, **90**, 1705 (1968).

(25) S. N. Ghosh, R. Trambarulo, and W. Gordy, *J. Chem. Phys.*, **21**, 308 (1953).

(26) P. S. Bryan and R. L. Kuczkowski, *J. Chem. Phys.*, **55**, 3049 (1971).

(27) Y. Morino, K. Kuchitsu, and T. Moritani, *Inorg. Chem.*, **8**, 867 (1969).

(28) C. A. Burrus, A. Jache, and W. Gordy, *Phys. Rev.*, **95**, 706 (1954).

(29) J. R. Durig, V. F. Kalasinsky, Y. S. Li, and J. D. Odom, *J. Phys. Chem.*, **79**, 468 (1975).

Contribution from the Technical University of Denmark,
Chemistry Department A, DK-2800 Lyngby, Denmark

Lower Oxidation States of Selenium. I. Spectrophotometric Study of the Selenium–Selenium Tetrachloride System in a Molten NaCl–$AlCl_3$ Eutectic Mixture at 150°

R. FEHRMANN, N. J. BJERRUM,* and H. A. ANDREASEN

Received February 4, 1975

AIC500756

Four different solvated selenium species with low positive oxidation states were prepared by reduction of dilute solutions of $SeCl_4$ in a NaCl–$AlCl_3$ (37:63 mol %) melt at 150° with elementary selenium. A statistical analysis of the spectrophotometric measurements of the resulting melts showed that the two higher oxidation states of these species were $+^1/_2$ and $+^1/_4$ (or $+^4/_{17}$) whereas no accurate value could be calculated for the two lower oxidation states. The most likely values, however, of these lower oxidation states were found to be $+^1/_6$ and $+^1/_8$. Spectra for the possible species Se_4^{2+}, Se_8^{2+}, Se_{12}^{2+}, and Se_{16}^{2+} were also calculated.

Introduction

It has been known for a long time that selenium in analogy with tellurium forms colored solutions in sulfuric acid.[1] A fairly recent investigation by Gillespie and coworkers has revealed that these colored solutions contain the Se_4^{2+} and Se_8^{2+} ions.[2] The results obtained by Corbett and coworkers[3] seem to indicate that the same two ions are formed in chloroaluminate melts. The structure of Se_4^{2+} in $Se_4(HS_2O_7)_2$ is square planar[4] and the structure of Se_8^{2+} in $Se_8(AlCl_4)_2$ is bicyclic.[5] In the present work the solute selenium species in a NaCl–$AlCl_3$